Journal Name RSCPublishing

**ARTICLE** 

This manuscript has been authored by UT-Battelle, LLC under Contract No. DE-AC05-00OR22725 with the U.S. Department of Energy. The United States Government retains and the publisher, by accepting the article for publication, acknowledges that the United States Government retains a non-exclusive, paid-up, irrevocable, world-wide license to publish or reproduce the published form of this manuscript, or allow others to do so, for United States Government purposes. The Department of Energy will provide public access to these results of federally sponsored research in accordance with the DOE Public Access Plan (http://energy.gov/downloads/doe-public-access-plan).

Cite this: DOI: 10.1039/x0xx00000x

# A Sodium-Aluminum Hybrid Battery

Xiao-Guang Sun, <sup>a\*</sup> Zhizhen Zhang, <sup>b</sup> Hongyu Guang, <sup>ac</sup> Craig A. Bridges, <sup>a</sup> Youxing Fang, <sup>ad</sup> Yong-Sheng Hu, <sup>b\*</sup> Gabriel M. Veith, <sup>e</sup> Sheng Dai <sup>ad\*</sup>

Received 00th January 2012, Accepted 00th January 2012

DOI: 10.1039/x0xx00000x

www.rsc.org/

Novel hybrid batteries are fabricated using an aluminum anode, a sodium intercalation cathode  $Na_3V_2(PO_4)_3$  (NVP), and a sodium/aluminum dual salt electrolyte based on NaAlCl4 and an eutectic mixture of 1-ethyl-3-methylimidazolium chloride (EMImC) and aluminum chloride. Cyclic voltammograms indicate that increasing the molar concentration of AlCl3 in the electrolyte is beneficial to high coulombic efficiency of aluminum deposition/stripping, which, unfortunately, results in lower coulombic efficiency of sodium extraction/insertion in the cathode. Therefore, EMImC-AlCl3 with a molar ratio of 1-1.1 is used for battery evaluation. The hybrid battery with 1.0 M NaAlCl4 exhibits a discharge voltage of 1.25 V and a cathodic capacity of 99 mAh g-1 under a current rate of C/10. In addition, the hybrid battery exhibits good rate performance and long cycling stability while maintaining a high coulombic efficiency of 98 %. It is also demonstrated that increasing salt concentration can further enhance the cycling performance of the hybrid battery. X-ray diffraction analysis of the NVP electrodes under different conditions confirms that the main cathode reaction is indeed the Na extraction/insertion. Based on all earth-abundant elements, the new Na-Al hybrid battery is very attractive for stationary and grid energy storage applications.

**Keyword:** Aluminum battery, Na<sub>3</sub>V<sub>2</sub>(PO<sub>4</sub>)<sub>3</sub>, sodium battery, hybrid battery, ionic liquid

# 1.Introduction

The rapid increase in energy demand coupled with environmental concerns over the use of fossil fuels and their limited resources have spurred great interest in energy harvesting from renewable sources such as wind and solar.<sup>1, 2</sup> However, the energy from renewable solar and wind are intermittent and unreliable, therefore, they must be stored in electric energy storage (EES) devices.<sup>3, 4</sup> Among various EES technologies, lithium ion batteries (LIBs) are the most mature technologies with high energy density, high coulombic efficiency and long cycle life. Unfortunately, their high cost and the unevenly distributed global lithium source are major concerns.<sup>5</sup> As a result, beyond lithium technologies based on cheap and naturally abundant elements such as sodium (Na), 6-9 magnesium (Mg), 10-19 calcium, 20, <sup>21</sup> and aluminum (Al) ion batteries <sup>22-27</sup> have been intensively studied during the last few years. Among different metals, Al is one of the most earth abundant elements, only second to silicon, resulting in its low price of \$0.52/kg, 100 times lower than Li. In addition, Al with three electrons redox couple has distinct advantage over one electron redox couple such as Li and Na and two electrons redox couple such as Mg and Ca, providing a high theoretical specific capacity of 2980 mAh g<sup>-1</sup> and a high volumetric capacity of 8040 mAh cm<sup>-3</sup>.

The development of rechargeable Al ion batteries has been hampered by the electrolyte and cathode materials. Due to the low reduction potential of Al (-1.68 V vs. SHE), aqueous electrolytes cannot be used when Al is being used as the anode, since hydrogen will be released before Al can be plated during the reduction process. On the other hand, without using Al as the anode, Al ion batteries could be cycled in aqueous electrolytes. <sup>28-30</sup> However, to fully take advantage of the earth-abundancy Al anode is essential for rechargeable Al batteries; therefore, non-aqueous electrolytes are required. The non-aqueous electrolytes used in commercial SIGAL and Hall-Héroult processes for Al deposition are not suitable for ambient rechargeable Al batteries because highly flammable alkylaluminum and extreme high temperature are used, respectively. 31, 32 As an alternative, ambient room temperature ionic liquids with high ionic conductivity and wide electrochemical windows are good candidates for rechargeable Al batteries. 33-37 Currently, the ionic liquids used for Al deposition are still based on mixtures of anhydrous AlCl<sub>3</sub> and organic halide salts discovered sixty years ago.<sup>38-41</sup> It has been confirmed that only the acidic mixtures show reversible Al deposition/stripping, which poses stringent requirement for the hardwares of the Al batteries, as it has been shown that corrosion was readily occurred to stainless steels. <sup>42</sup> To avoid the corrosion issue, pouch cell and special cell configuration have been used. <sup>22, 43</sup> Recently, there are some new developments on Al deposition in ionic liquid electrolytes. <sup>44,55</sup> However, the suitability of these electrolytes for Al batteries still needs to be confirmed, especially their compatibility with new cathode electrode materials. Besides electrolytes, Al batteries also face challenges from the cathodes due to the high charge density of the Al<sup>3+</sup> ion, making its insertion/extraction into/from the cathode host very difficult. <sup>56</sup> Although different materials such as V<sub>2</sub>O<sub>5</sub>, <sup>42, 57, 58</sup> VO<sub>2</sub>, <sup>59</sup> Mo<sub>6</sub>S<sub>8</sub>, <sup>60, 61</sup> copper hexacyanoferrate, <sup>29, 62</sup> conducting polymers, <sup>63</sup> and fluorinated graphite <sup>64</sup> have been evaluated as cathodes for Al batteries, low cell voltage and poor cycling performance were usually observed. Recently, high voltage Al batteries with good cycling performance were reported by utilizing three-dimensional graphitic-foam and carbon paper as cathodes. <sup>22, 65</sup>

An alternative way to take advantage of metallic Al anode but bypasses the need for efficient Al insertion cathodes is hybrid Al battery.43 It was demonstrated that high voltage and high capacity were possible in a hybrid Al battery with LiFePO4 as the cathode in an acidic ionic liquid electrolyte. 43 However, considering the limited Li resources, a switch to the more earth-abundant sodium chemistry is more desirable. Based on the same consideration new Na-Mg hybrid batteries have been reported recently.<sup>66,67</sup> Herein, we report a new hybrid battery using earth-abundant Na and Al chemistry, that is, Al as the anode, Na<sub>3</sub>V<sub>2</sub>(PO<sub>4</sub>)<sub>3</sub> (NVP) as the cathode and NaAlCl<sub>4</sub> dissolved in acidic ionic liquid as the electrolyte. The selection of NVP as the cathode is based on the fact that it is also composed of earth-abundant elements, has flat charge/discharge plateaus and fast Na extraction/insertion characteristics.<sup>68-71</sup> It should also be emphasized that NVP is used to demonstrate the concept of new hybrid Al battery and investigate its working mechanism, its limitation on capacity and cell voltage can be easily improved by selecting other suitable high capacity and high voltage cathode materials.

Fig. 1a illustrates the working principle of the hybrid Al battery, that is, during the charge/discharge process, the anode reaction is reversible Al deposition/stripping while the cathode reaction is Na extraction/insertion, respectively. The overall cell reactions can be described by the following equations:

Anode:  $8NaAl_2Cl_7 + 6Na^+ + 6e^- \leftrightarrow 2Al + 14NaAlCl_4$ 

Cathode:  $3Na_3V_2(PO_4)_3 - 6e^- \leftrightarrow 3NaV_2(PO_4)_3 + 6Na^+$ 

Overall:  $8NaAl_2Cl_7 + 3Na_3V_2(PO_4)_3 \leftrightarrow 2Al + 14NaAlCl_4 + 3NaV_2(PO_4)_3$ 

Fig.1b illustrates the specially designed polyethylene inner cup placed inside the coin cell that is bridged with Pt wire to avoid the corrosion of the ionic liquids toward the coin cell cases. <sup>43</sup>

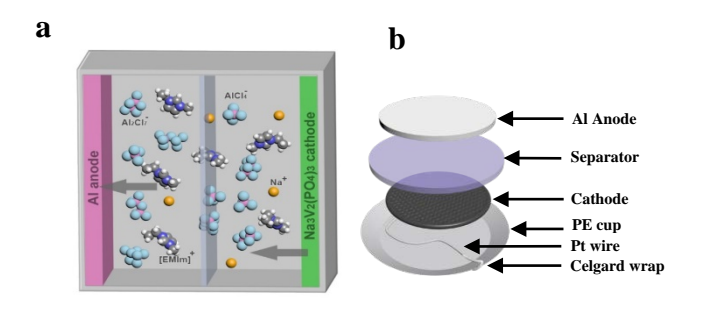


**Fig. 1.** a) Schematic illustration of the hybrid battery with Al as the anode,  $Na_3V_2(PO_4)_3$  as the cathode and  $NaAlCl_4$  dissolved in acidic ionic liquid as the electrolyte; b) internal coin cell design that mitigates the corrosion issue of acidic electrolyte towards the stainless steel cases of the coin cell.

## 2. Results and discussion

#### 2.1. Ionic conductivity

It has been demonstrated previously that when the molar ratio of EMImC-AlCl<sub>3</sub> was 1-1.1, reversible Al deposition/stripping was possible.<sup>43</sup> In this work, a more acidic electrolyte with a molar ratio of EMImC-AlCl<sub>3</sub> being 1-1.3 was also prepared and evaluated. Fig. 2 shows the temperature dependence of the ionic conductivities of the electrolytes with and without NaAlCl<sub>4</sub>. Generally, the temperature dependence of the ionic conductivities can be described by the well-known Vogel–Fulcher–Tamman (VFT) equation:<sup>72-74</sup>

$$\sigma = \sigma_0 \exp[-B/(T - T_0)] \tag{1}$$

where  $\sigma_0$  (S cm<sup>-1</sup>) is a constant, B (K) is the pseudo-activation energy, and  $T_0$  (K) is the vanishing ion mobility temperature. As demonstrated in Fig. 2, the ionic conductivities of the electrolytes with NaAlCl<sub>4</sub> are lower than those without it, mainly due to the higher viscosities of the former solutions. <sup>37</sup> It is also observed that the electrolytes based on EMImC-AlCl<sub>3</sub> (1-1.3), with or without NaAlCl<sub>4</sub>, are much higher than those based on EMImC-AlCl<sub>3</sub> (1-1.1). The ionic conductivities at 20 °C are 1.41 x  $10^{-2}$ , 9.32 x  $10^{-3}$ , 1.83 x  $10^{-2}$ , and 9.90 x  $10^{-3}$  S cm<sup>-1</sup> for EMImC-AlCl<sub>3</sub> (1-1.1), 1.0 M NaAlCl<sub>4</sub>/ EMImC-AlCl<sub>3</sub> (1-1.1), EMImC-AlCl<sub>3</sub> (1-1.3), and 1.0 M NaAlCl<sub>4</sub>/ EMImC-AlCl<sub>3</sub> (1-1.3), respectively. These ionic conductivities are high enough for practical battery applications.

### 2.2. Cyclic Voltammograms

Figs. 3a and 3b show the cyclic voltammograms (CVs) of the ionic liquid electrolyte EMImC-AlCl<sub>3</sub>(1-1.1) with and without NaAlCl<sub>4</sub> on a Pt working electrode at a scan rate of 20 mV/s. Reversible Al deposition/stripping is still observed after addition of NaAlCl<sub>4</sub>, similar to the case of LiAlCl<sub>4</sub> being added in the hybrid Al/LiFePO<sub>4</sub> battery. Typical aluminum nucleation loops are observed in both electrolyte solutions during the reduction process with significant overpotentials. The current densities of the electrolytes with NaAlCl<sub>4</sub> are always lower than those without NaAlCl<sub>4</sub>, mainly due to their lower ionic conductivities (Fig.3 and Fig.S1 in the ESI). In addition, the current densities of the

electrolytes based on EMImC-AlCl<sub>3</sub> (1-1.3) (Fig. S1 in the ESI) are higher than those based on EMImC-AlCl<sub>3</sub> (1-1.1), probably due to the presence of more active Al<sub>2</sub>Cl<sub>7</sub> species. Table 1 summarizes the coulombic efficiencies of Al deposition/stripping in both EMImC-AlCl<sub>3</sub> (1-1.1) and EMImC-AlCl<sub>3</sub> (1-1.3) electrolytes, with and without NaAlCl<sub>4</sub>. It is noticed that the coulombic efficiencies of the electrolytes containing NaAlCl<sub>4</sub> are similar to those without it. However, the coulombic efficiencies of the electrolytes based on EMImC-AlCl<sub>3</sub> (1-1.3) are always higher than those based on EMImC-AlCl<sub>3</sub> (1-1.1). These CV results indicate that at least on an inert working electrode (Pt), the more acidic electrolyte is beneficial to high coulombic efficiency of aluminum deposition/stripping.

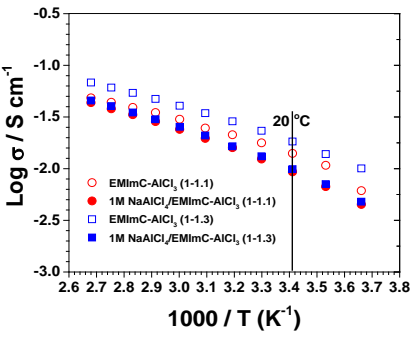


**Fig. 2.** Temperature dependence of ionic conductivities of the acidic ionic liquid electrolytes, EMImC-AlCl<sub>3</sub>(1-1.1), 1M NaAlCl<sub>4</sub>/EMImC-AlCl<sub>3</sub>(1-1.1), EMImC-AlCl<sub>3</sub>(1-1.3) and 1M NaAlCl<sub>4</sub>/EMImC-AlCl<sub>3</sub> (1-1.3).

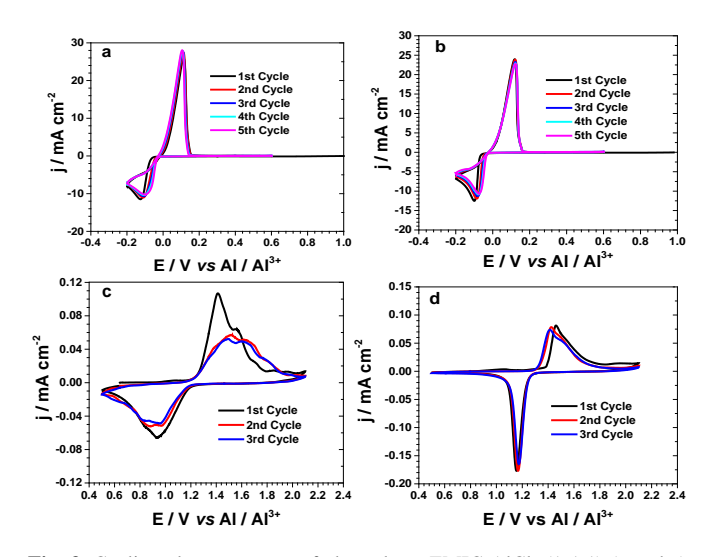


**Fig. 3.** Cyclic voltammograms of electrolytes EMIC-AlCl<sub>3</sub> (1-1.1) (a and c) and 1.0 M NaAlCl<sub>4</sub>/EMIC-AlCl<sub>3</sub> (1-1.1) (b and d) on a Pt (a and b) and NVP (c and d) electrodes at a scan rate of 20 mV/s (a and b) and 0.1mV/s (c and d), respectively.

**Table 1** Coulombic efficiencies of Al deposition/stripping on a Pt working electrode in different ionic liquid electrolytes.

Electrolyte	1 <sup>st</sup> cycle	2 <sup>nd</sup> cycle	3 <sup>rd</sup> cycle	4 <sup>th</sup> cycle	5 <sup>th</sup> cycle
EMIC-AlCl <sub>3</sub> (1-1.1)	92.0	93.4	94.6	94.2	93.8
1.0 M NaAlCl <sub>4</sub> /EMIC- AlCl <sub>3</sub> (1-1.1)	91.5	93.3	93.3	93.9	93.5
EMIC-AlCl <sub>3</sub> (1-1.3)	97.2	97.3	98.1	94.9	95.1
1.0M NaAlCl <sub>4</sub> /EMIC-	95.8	95.5	96.0	95.8	96.1

AlCl<sub>3</sub> (1-1.3)

Figs. 3c and d show the CVs of the Na<sub>3</sub>V<sub>2</sub>(PO<sub>4</sub>)<sub>3</sub> (NVP) electrode in the EMIC-AlCl<sub>3</sub> (1-1.1) electrolyte, with and without NaAlCl<sub>4</sub>, at a scan rate of 0.1 mV/s. It is noted that the CVs with NaAlCl4 are significantly different from those without it, which are also dramatically different from those observed in the hybrid Al||LiFeO<sub>4</sub> battery.<sup>43</sup> There is no significant polarization during the initial sodium extraction process for the electrolyte without NaAlCl4. Even though they both have two oxidation peaks for Na<sup>+</sup> extraction process, there is only one sharp reduction peak in the electrolyte with NaAlCl<sub>4</sub> for Na<sup>+</sup> insertion process. In addition, the polarization in the electrolyte without NaAlCl4 increases with cycling, as evidenced by the downshift of the reduction peaks and upshift of the oxidation peaks with cycling (Fig. 3c). Similar trends are also observed for the EMIC-AlCl<sub>3</sub> (1-1.3) electrolyte with and without NaAlCl<sub>4</sub> (Fig. S1 in the ESI). Table 2 summaries the coulombic efficiencies of the first five cycles of the NVP cathode in both EMImC-AlCl<sub>3</sub> (1-1.1) and EMImC-AlCl<sub>3</sub> (1-1.3) electrolytes, with and without NaAlCl<sub>4</sub>. Generally, the coulombic efficiencies of the two electrolytes with NaAlCl4 are much higher than those without it. However, the coulombic efficiencies of EMIC-AlCl<sub>3</sub> (1-1.1) based electrolytes are higher than those of EMIC-AlCl<sub>3</sub> (1-1.3) based electrolytes. This result is in direct contrast to the behaviour obtained on the Pt electrode (Table 1), indicating that the electrolytes based on the stronger acid EMIC-AlCl<sub>3</sub> (1-1.3) might initiate some side reactions on the cathode. Therefore, the battery evaluation is mainly focused on the less acidic electrolyte EMIC-AlCl<sub>3</sub> (1-1.1). For comparison, the battery performance using the stronger acid EMIC-AlCl<sub>3</sub> (1-1.3) based electrolytes is provided in the ESI section.

## 2.3. Cell performance

Fig. 4a shows the typical charge-discharge profile of a hybrid battery in the electrolyte of 1.0 M NaAlCl<sub>4</sub>/EMIC-AlCl<sub>3</sub> (1-1.1) at different current rates. As expected from previous CV studies, the charge profile shows an apparent two-step process while the discharge profile exhibits a single step. The potential polarization between the first charge step and the discharge curve under the current densities of C/10 and C/5 is only 60 mV, which increases to 100 mV, 160 mV and 260 mV under the current density of C/2, 1C and 2C, respectively. The initial low polarization between charge and discharge is similar to that observed in organic electrolyte, 70 but different from those observed in the hybrid Al||LiFePO4 batteries, indicating facile ion insertion/extraction into/from the Na<sub>3</sub>V<sub>2</sub>(PO<sub>4</sub>)<sub>3</sub> cathode. However, it should be noted that double active material loading was used in the organic electrolyte based cell tests.<sup>70</sup> Nonetheless, high charge and discharge capacities of 106.9 and 98.9mAh g<sup>-1</sup> are obtained under a current density of C/10, resulting in a high initial coulombic efficiency of 92.5. %. The charge and discharge capacities decrease to 96.9 and 94.6 mAh g<sup>-1</sup> under C/5, 91.9 and 89.3 mAh g<sup>-1</sup> under C/2, 82.3 and 80.1 mAh g<sup>-1</sup> under 1C, and 69.1 and 67.8 mAh g<sup>-1</sup> under 2C, respectively. Considering the good rate performance in Fig. 4b, a fresh hybrid battery was assembled and evaluated under a current rate of C/5. The initial reversible capacity is 86 mAh g<sup>-1</sup>, and it reduces to 69 mAh g<sup>-1</sup> after 100 cycles, resulting in a capacity retention of 80 % (Fig. 4d). The initial gradual decrease of the capacity is similar to that observed in the hybrid Al||LiFePO4 battery, which is attributed to the trapping of sodium in the electrolyte.<sup>43</sup> For comparison, a hybrid battery using pure EMImCl-AlCl<sub>3</sub> (1-1.1) electrolyte was assembled and cycled under the same current density of C/5. As shown in Fig.S2a in the ESI, the initial potential polarization between charge and discharge curve is 180 mV, which increases with cycling and it is as high as 480 mV after 50 cycles. Also, under the same current rate of C/5 the

polarization is much worse when the stronger acid electrolyte EMIC-AlCl<sub>3</sub> (1-1.3) is used (Fig. S2c in the ESI). The increasing polarization with cycling in the electrolyte without NaAlCl4, as compared to the low polarization observed in the electrolyte with NaAlCl<sub>4</sub> (Fig.4c), confirms the severe trapping of Na<sup>+</sup> in the former. The trapping of Na+ in the electrolyte without NaAlCl4 also contributes to the quick capacity drop in the first few cycles as well as the following slow capacity degradation (Figs. S2b and S2d in the ESI). It is further evidenced by the high coulombic efficiencies (98 %) for the batteries with NaAlCl4 (Fig. 4b and d) versus low coulombic efficiencies (less than 90 %) for those without NaAlCl4(Figs. S2b and S2d). On the other hand, if 1.0 M NaAlCl<sub>4</sub>/EMIC-AlCl<sub>3</sub> (1-1.3) is used to assemble hybrid battery; a low polarization of 120 mV is maintained throughout the cycling process (Fig. S3a in the ESI), however, the coulombic efficiency decreases from the initial 97 % to only 94 % after 50 cycles (Fig. S3b in the ESI). The low coulombic efficiency is mainly due to the aforementioned side reactions resulting from the stronger acid electrolyte.

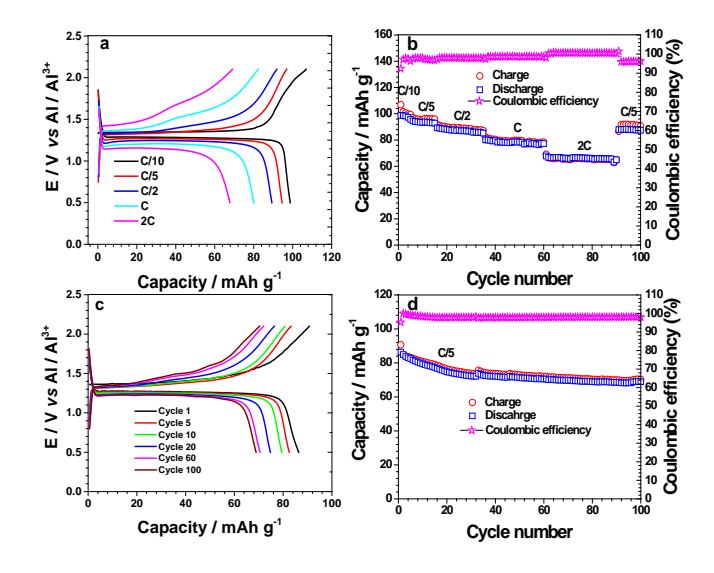


**Fig. 4.** Charge/discharge profile (a and c) and cycling stability (b and d) of the hybrid battery Al||NVP in 1.0 M  $NaAlCl_4/EMIC-AlCl_3$  (1-1.1) at different current rates and cycles, respectively. (The active material loading for Fig. 4a and 4b is 1.4 mg/cm<sup>2</sup> while that for Fig. 4c and d is 2.0 mg/cm<sup>2</sup>).

**Table 2** Coulombic efficiencies of Na insertion/extraction in NVP<sub>3</sub> cathode in different ionic liquid electrolytes.

Electrolyte	1 <sup>st</sup> cycle	2 <sup>nd</sup> cycle	3 <sup>rd</sup> cycle	4 <sup>th</sup> cycle	5 <sup>th</sup> cycle
EMIC-AlCl <sub>3</sub> (1-1.1)	73.9	88.4	91.6	92.8	92.8
1.0 M NaAlCl <sub>4</sub> /EMIC- AlCl <sub>3</sub> (1-1.1)	80.0	92.0	94.4	94.1	94.1
EMIC-AlCl <sub>3</sub> (1-1.3)	65.5	81.1	82.8	84.4	82.6
1.0M NaAlCl <sub>4</sub> /EMIC- AlCl <sub>3</sub> (1-1.3)	83.7	90.2	91.4	91.0	91.0

To reduce the trapping of Na<sup>+</sup> with cycling while maintaining high coulombic efficiency, a high salt concentration electrolyte, 2.0 M NaAlCl<sub>4</sub>/EMIC-AlCl<sub>3</sub> (1-1.1), was used to assemble the hybrid battery that was cycled under the same current density of C/5. As shown in Fig.5, a low polarization of 60 mV is maintained

throughout the cycling process. In addition, the capacity quickly reaches equilibrium within the first 10 cycles, whereas it takes more than 20 cycles to reach equilibrium for the cell using 1.0 M NaAlCl4 electrolyte (Fig. 4d). Furthermore, a high coulombic efficiency of 98.5 % and high capacity retention are realized with the use of high concentration electrolyte. For example, the initial reversible capacity in 2.0 M NaAlCl4 electrolyte is 96.3 mAh g<sup>-1</sup>, and it reduces to 85.6 mAh g<sup>-1</sup> after 50 cycles, resulting in capacity retention of 88.9 % (Fig. 5b). In contrast, the capacity retention for the cell in 1.0 M NaAlCl4 electrolyte is only 82.6 % after 50 cycles (Fig.4d). The above result confirms that high salt concentration is an effective way to reduce the trapping of Na<sup>+</sup> and improve long cycle stability while maintaining high coulombic efficiency in the new hybrid Al battery.

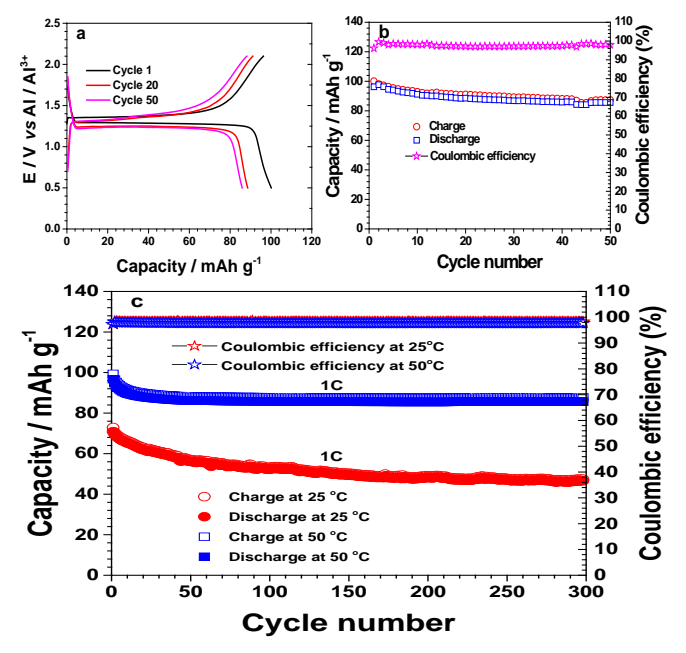


Fig. 5. Charge/discharge profile (a) and cycling stability (b) of the hybrid battery  $Al||Na_3V_2(PO_4)_3$  in 2.0 M  $NaAlCl_4/EMIC-AlCl_3$  (1-1.1) at the current rate of C/5 (The active material loading is 1.2 mg/cm<sup>2</sup>); (c) cycling stability of the hybrid battery in 2.0 M  $NaAlCl_4/EMIC-AlCl_3$  (1-1.1) at a current rate of 1C at 25 and 50 °C (The active material loading is 1.1 mg/cm<sup>2</sup>).

To further demonstrate the potential of the hybrid battery, its cycling stability was studied up to 300 cycles at a high current rate of 1 C. At 25 °C, the reversible capacity slowly decays from initial 71 mAh g<sup>-1</sup> to 48 mAh g<sup>-1</sup> after 300 cycles. The capacity decay can be attributed to the high current rate and low ionic conductivity of the ionic liquid electrolyte, as the cycling stability is significantly improved when a similar hybrid battery was cycled at 50 °C. For example, the cell has an initial high capacity of 98.3 mAh g<sup>-1</sup>, and it slowly decreases only within the first 20 cycles to 88 mAh g<sup>-1</sup> however, it is still as high as 86 mAh g<sup>-1</sup> after 300 cycles. The coulombic efficiency is 98.3 % for the hybrid battery cycled at 25 °C while it is 97.8 % for the one cycled at 50 °C. The charge-discharge profiles of the two hybrid batteries for the first cycle and the 300th cycle are compared in Fig. S6. Apparently, the cell polarization is more severe at 25 °C than at 50 °C, especially at the end of the cycling.

## 2.4. Cell working mechanism investigation

To confirm the potential observed in the hybrid Al batteries is truly related to Na extraction/insertion from/into the NVP cathode, X-ray diffraction (XRD) analysis was used to follow the reaction of the cathode. Na||NVP half-cells using Swagelok were first assembled in the electrolyte of 1.0 M NaClO<sub>4</sub>/ethylene carbonate (EC)diethylene carbonate (DEC) (1/1, by Vol), which was charged under a constant current of 19.3 µA until the voltage reaches 3.7 V vs Na/Na+. As shown in Fig. 6a, there is a flat plateau at 3.4 V vs Na/Na<sup>+</sup>, same as those reported in the literature. <sup>70, 71</sup> The Swagelok cells were then disassembled inside the glovebox and the electrodes were washed with anhydrous dimethyl carbonate (DMC) for three times, followed by drying under vacuum for overnight. Hybrid Al||NaV2(PO4)3 cells were then assembled in the ionic liquid electrolyte of 1.0 M NaAlCl<sub>4</sub>/ EMIC-AlCl<sub>3</sub> (1-1.1). The cells usually exhibit an open cell voltage of 1.45 V vs Al/Al3+, indicating that the electrochemical potential of the hybrid cells are less than 1.45 V. Indeed, as shown previously and in Fig. 6b, there is a flat discharge plateau at 1.27 V vs Al/Al<sup>3+</sup>. The coulombic efficiency between Na insertion in the ionic liquid electrolyte (Fig. 6b) and Na extraction in the carbonate electrolyte (Fig. 6a) is 90.8%. On the other hand, the coulombic efficiency of Na extraction and insertion in the ionic liquid electrolyte (Fig. 6b) is 100%. Other samples involving Na extraction in the carbonate electrolyte and Na insertion in the ionic liquid electrolyte are shown in Fig.S4 and S5, respectively.

Fig. 6c shows the XRD patterns of the NVP electrode under different conditions. The diffraction peaks of the pristine NVP electrode are the same as that of the starting NVP powder, though the pattern contains a strong contribution from the carbon cloth. The XRD peaks at 14.6°, 20.5°, 21.5°, 24.6°, 29.6° and 32.8° for Na extraction in the carbonate electrolyte are consistent with prior reports of the Na|| NVP battery,70 which can be indexed to NaV<sub>2</sub>(PO<sub>4</sub>)<sub>3</sub>, confirming that Na is indeed being extracted. Furthermore, the XRD patterns for Na insertion in the ionic liquid electrolyte are same as those of the fresh electrode. More importantly, the XRD patterns for Na extraction in the ionic liquid electrolyte are same as those for Na extraction in the carbonate electrolyte. Finally, the XRD patterns of the electrode cycled for 50 cycles are same as those of the pristine electrode, indicating the cathode structure is well maintained after long cycling. The above XRD spectra confirm that the main cathode reaction observed in the hybrid Na||Al battery is indeed the Na extraction/insertion from/into the NVP host.

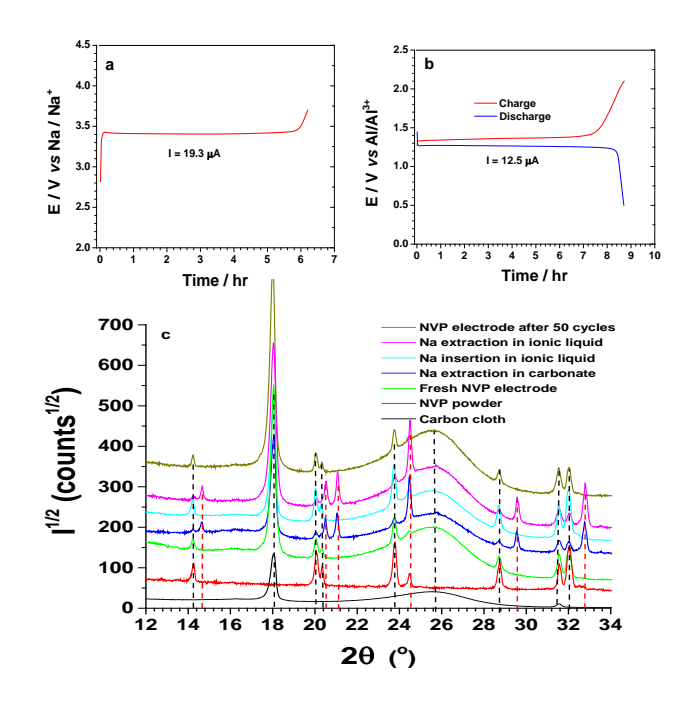


**Fig. 6** (a) Sodium extraction profile of Na  $\parallel$  NVP Swagelok cell in 1.0 M NaClO<sub>4</sub>/EC-DEC under a current of 19.3  $\mu$ A; (b) Charge/discharge profile of hybrid Al $\parallel$ NVP cell in 1.0 M NaAlCl<sub>4</sub>/EMIC-AlCl<sub>3</sub> (1-1.1) under a current of 12.5  $\mu$ A;(c) XRD patterns of the NVP electrodes under different conditions as specified in the figure caption. Black dashed lines correspond to sodiated NVP, red dashed lines correspond to desodiated NVP. Several other peaks are present that can be assigned to the carbon cloth.

In summary, we have demonstrated the first hybrid battery based on the chemistry of Na and Al, which can achieve high capacity and high coulombic efficiency in an electrolyte based on NaAlCl<sub>4</sub> and a low acidic ionic liquid EMIC-AlCl<sub>3</sub> (1-1.1, in molar). The safe nature and earth abundance of both sodium and aluminum, coupled with high safety of the ionic liquid electrolytes makes this new hybrid battery very attractive for grid and stationary applications. Even though the energy density of the current hybrid battery is very low as compared to the rocking-chair batteries due to low capacity and low potential of the NVP electrode as well as larger amount of the electrolyte being used, 75 it will become more favourable and competitive if high capacity Na+ insertion cathodes with potentials above 2.0 V vs Al/Al3+ and corresponding high voltage ionic liquid electrolytes can be developed. A close relative to NVP is the fluorinated version, Na<sub>3</sub>V<sub>2</sub>(PO<sub>4</sub>)F<sub>3</sub>, which shows both high voltage and capacity than NVP.<sup>76-80</sup>

### **Conclusions**

In summary, we have demonstrated the first hybrid battery based on the chemistry of Na and Al in an electrolyte of NaAlCl4 dissolved in a low acidic ionic liquid of EMIC-AlCl<sub>3</sub> (1-1.1). The hybrid battery with 1.0 M NaAlCl4 exhibits a discharge voltage of 1.25 V and a cathodic capacity of 99 mAh g<sup>-1</sup> under a current rate of C/10. Even though the energy density of the current hybrid battery is only 124 Wh kg<sup>-1</sup>, which cannot compete with current state-of-art lithium ion batteries, the safe nature and earth abundance of both sodium and aluminum, coupled with the high safety of ionic liquid electrolytes still make this new kind of hybrid battery very attractive for grid and stationary applications. Particularly, if suitable Na+ insertion cathodes with high capacity of 150 mAh g-1 and an operation potential around 2.0 V versus Al/Al3+ can be developed, the energy density of the corresponding hybrid battery will be increased to 300 Wh kg-1, which can significantly increase its capability for grid and stationary applications.

## 3. Experimental Section

#### 3.1. Materials

Anhydrous Al chloride (AlCl<sub>3</sub>) was purchased from Fluka and was purified by sublimation. High purity sodium chloride (99.5%) was purchased from Aldrich and dried at 200 °C for overnight. Equal molar mixture of purified AlCl<sub>3</sub> and dried NaCl were mixed inside the glovebox and transferred to a Pyrex glass tube, which was then taken outside the glovebox and sealed under vacuum with a torch. The tube was heated to 240 °C inside an oven until it becomes a clear solution. After cooling to room temperature, NaAlCl<sub>4</sub> was grinded inside the glovebox and was used to prepare the electrolyte solutions. 1-ethyl-3-methylimidazolium chloride (EMImC) was purchased from Aldrich and purified via repeated recrystallization according to the reported procedure.<sup>38</sup> NaClO<sub>4</sub> monohydrate was purchased from Aldrich and was dried at 150 °C under vacuum for 24 hours before use. Anhydrous propylene carbonate (PC) was purchased from Novolyte Inc and was used directly. 1.0 M NaClO<sub>4</sub>/ PC solution was prepared inside the glove box. Na<sub>3</sub>V<sub>2</sub>(PO<sub>4</sub>)<sub>3</sub> was synthesized according to the reported procedure. 70, 71 Different molar ratios of AlCl<sub>3</sub> to EMImC, as well as different concentrations of NaAlCl<sub>4</sub> in the acidic ionic liquids, were prepared inside the glovebox.

#### 3.2 Electrochemical Measurement

High purity Al foil and wire (99.99%) from Aldrich were used as anode and reference electrode, respectively. Al foil was cut into disks with diameters of 1.1 cm. The Al disks were mechanically polished with fine sandpaper, followed by activation in an acidic solution composed of 1 wt. % HNO<sub>3</sub>, 65 wt. % H<sub>3</sub>PO<sub>4</sub>, 5 wt. % acetic acid and water for 5 min. Finally, they were rinsed thoroughly with deionized water and degreased in acetone for 5 min before taking inside the glove box (moisture and oxygen level below 0.5 ppm) for cell assembling.

The cathode was fabricated by casting a slurry of Na<sub>3</sub>V<sub>2</sub>(PO<sub>4</sub>)<sub>3</sub> carbon wt.%), Super-S black (20 wt.%), polytetrafluoroethylene (PTFE, 10 wt.%) in a mixture of methanol/water (1/1, in V) onto E-Tek carbon cloth. Solvent was removed and the electrodes were cut into discs with a diameter of 1.1 cm and further dried in a vacuum oven at 110 °C overnight. The active material loading was 1.0 - 2.0 mg/cm<sup>2</sup>. The coin cells were assembled with Na<sub>3</sub>V<sub>2</sub>(PO<sub>4</sub>)<sub>3</sub> as cathode, Al disk as both counter and reference electrode, and glass fibre paper soaked with the electrolyte as separator. To avoid corrosion of the coin cell parts, a special cell design as shown in Fig. 1b was adopted, 43 that is, an insulating shallow cup made of polyethylene was used as an internal container for the cathode electrode and the acidic electrolyte soaked in carbon fibre paper. The cup was designed to fit inside the coin cell sealing gasket. A thin platinum wire was used as a bridge between the cathode and the coin cell base. To avoid shorting of the coin cell during cramping, the wire was wrapped with Celgard at the edge of the cup. Finally, a fixed amount of 80  $\square$ 1 electrolyte was used to assemble the coin cells, which was enough to wet the cathode and the separator but avoided flooding the shallow cup.

The ionic conductivity was measured by AC impedance spectroscopy using a Biologic VMP potentiostat in the frequency range from  $2 \times 10^5$  Hz to 1 Hz with a perturbation amplitude of 10 mV. 37 The conductivity measurement was carried out in a self-made conductivity cell with two parallel glass-sealed platinum electrodes. The cell was placed in an aluminum block that was heated from room temperature to 100°C, with equilibration time of 30 min at each measuring temperature. The cell constants were calibrated with a 0.1 M KCl aqueous standard solution at 25°C. Cyclic voltammetry (CV) was performed on the Biologic instrument using either twoelectrode or three electrode configuration. The electrochemical behaviour of Al anode in the acidic ionic liquids was investigated using Pt as working electrode, Al coil and Al wire as counter and reference electrode, respectively. The electrochemical behaviour of the Na<sub>3</sub>V<sub>2</sub>(PO<sub>4</sub>)<sub>3</sub> cathode was investigated using coin cells. The CVs were recorded at a scan rate of 20 mV/s on Pt electrode and 0.1 mV/s on Na<sub>3</sub>V<sub>2</sub>(PO<sub>4</sub>)<sub>3</sub> in the voltage range of - 0.2 - 0.6 V and 0.5 V-2.1 V vs. Al/Al<sup>3+</sup>, respectively. The battery cycling performance was evaluated using an Arbin BT2000 instrument. The cells were charged and discharged under different current rates, according to the theoretical capacity of Na<sub>3</sub>V<sub>2</sub>(PO<sub>4</sub>)<sub>3</sub> (117 mAh g<sup>-1</sup>). <sup>70, 71</sup> The cut off voltages were 0.5 V and 2.1 V during discharge and charge, respectively.

XRD patterns were collected on a Panalytical Empyrian X-ray diffractometer using Cu  $K_{\alpha}$  radiation. Due to slight differences in each carbon cloth it was observed that there were slight height offsets. Therefore, the patterns as presented in Figure 6 have been corrected against the main peak position of the carbon cloth, for ease of comparison. For XRD analysis the Na||NVP half-cells were assembled using a carbonate electrolyte of 1.0 M NaClO<sub>4</sub>/EC-DEC (1/1, by Vol). The half-cells were charged under a constant current

of 19.3  $\mu A$  until the voltage reaches 3.7 V vs. Na/Na<sup>+</sup>, after which the cells were disassembled inside the glove-box and the electrodes were washed with dry DMC for three times. After drying the electrodes were then used to assemble Al||NaV<sub>2</sub>(PO<sub>4</sub>)<sub>3</sub> half-cells, which were discharged and charged, respectively. Finally, these cells were disassembled inside the glove-box and washed with dry toluene for three times and dried under vacuum before analysis.

#### Acknowledgements

This research was supported by the U.S. Department of Energy's Office of Science, Basic Energy Science, Materials Sciences and Engineering Division.

Received: ((will be filled in by the editorial staff))
Revised: ((will be filled in by the editorial staff))
Published online: ((will be filled in by the editorial staff))

#### **Notes and references**

- <sup>a</sup> Chemical Sciences Division, Oak Ridge National Laboratory, One Bethel Valley Road, Oak Ridge, TN 37831, USA
- Emails: sunx@ornl.gov; dais@ornl.gov
- b Key Laboratory for Renewable Energy, Institute of Physics, Chinese Academy of Sciences
- Zhongguancun South 3rd Street No.8, Beijing 100190, P. R. China Email: yshu@aphy.iphy.ac.cn
- <sup>c</sup> Department of Chemistry, Northeast Normal University, 5268 Renmin Street, Changchun, Jilin 130012, P. R. China
- <sup>d</sup> Department of Chemistry, University of Tennessee, Knoxville, Tennessee 37996, USA
- <sup>e</sup> Materials Science and Technology Division, Oak Ridge National Laboratory, One Bethel Valley Road, Oak Ridge, TN 37831, USA
- † Footnotes should appear here. These might include comments relevant to but not central to the matter under discussion, limited experimental and spectral data, and crystallographic data.

Electronic Supplementary Information (ESI) available: [Cyclic voltammograms, charge-discharge profile, and cycling stability of hybrid batteries]. See DOI: 10.1039/b000000x/

- Z. G. Yang, J. L. Zhang, M. C. W. Kintner-Meyer, X. C. Lu, D. W. Choi, J. P. Lemmon and J. Liu, *Chem. Rev.*, 2011, 111, 3577-3613.
- 2. J. B. Goodenough, H. D. Abruna and M. V. Buchanan, *Basic Research Needs for Electrical Energy Storage*, 2007.
- 3. D. Larcher and J. M. Tarascon, Nature Chem., 2015, 7, 19-29.
- 4. B. Dunn, H. Kamath and J. M. Tarascon, Science, 2011, 334, 928-935.
- H. L. Pan, Y. S. Hu and L. Q. Chen, Energy Environ. Sci., 2013, 6, 2338-2360.
- B. L. Ellis and L. F. Nazar, Curr Opinion Solid State Mater Sci., 2012, 16, 168-177.
- S. W. Kim, D. H. Seo, X. H. Ma, G. Ceder and K. Kang, Adv. Energy Mater., 2012, 2, 710-721.
- N. Yabuuchi, K. Kubota, M. Dahbi and S. Komaba, Chem. Rev., 2014, 114, 11636-11682.
- J. Liu, J. G. Zhang, Z. G. Yang, J. P. Lemmon, C. Imhoff, G. L. Graff, L. Y. Li, J. Z. Hu, C. M. Wang, J. Xiao, G. Xia, V. V. Viswanathan, S. Baskaran, V. Sprenkle, X. L. Li, Y. Y. Shao and B. Schwenzer, *Adv. Funct. Mater.*, 2013, 23, 929-946.
- P. Saha, M. K. Datta, O. I. Velikokhatnyi, A. Manivannan, D. Alman and P. N. Kumta, *Prog. Mater. Sci.*, 2014, 66, 1-86.
- 11. R. Mohtadi and F. Mizuno, Beilstein J. anotech., 2014, 5, 1291-1311.
- J. Muldoon, C. B. Bucur and T. Gregory, *Chem. Rev.*, 2014, **114**, 11683-11720.
   H. D. Yoo, J. Shtaraphora, V. Cofar, C. Cambinelly, N. Pour, and D.
- 13. H. D. Yoo, I. Shterenberg, Y. Gofer, G. Gershinsky, N. Pour and D. Aurbach, *Energy Environ. Sci.*, 2013, **6**, 2265-2279.
- Y. Cheng, Y. Shao, Z. Ji-Guang, V. L. Sprenkle, J. Liu and G. Li, *Chem. Commun.*, 2014, 50, 9644-9646.
- T. Liu, Y. Shao, G. Li, M. Gu, J. Hu, S. Xu, Z. Nie, X. Chen, C. Wang and J. Liu, *J Mater. Chem. A*, 2014, 2, 3430-3438.

 T. Gao, F. Han, Y. Zhu, L. Suo, C. Luo, K. Xu and C. Wang, Adv. Energy Mater., 2015, 5, 1401507.

- H. S. Kim, T. S. Arthur, G. D. Allred, J. Zajicek, J. G. Newman, A. E. Rodnyansky, A. G. Oliver, W. C. Boggess and J. Muldoon, *Nature Commun.*, 2011, 2, 427.
- D. Aurbach, Z. Lu, A. Schechter, Y. Gofer, H. Gizbar, R. Turgeman, Y. Cohen, M. Moshkovich and E. Levi, *Nature*, 2000, 407, 724-727.
- Z. X. Feng, X. Chen, L. Qiao, A. L. Lipson, T. T. Fister, L. Zeng, C. Kim, T. H. Yi, N. Sa, D. L. Proffit, A. K. Burrell, J. Cabana, B. J. Ingram, M. D. Biegalski, M. J. Bedzyk and P. Fenter, ACS Appl. Mater. Interfaces, 2015, 7, 28438-28443.
- A. Ponrouch, C. Frontera, F. Barde and M. R. Palacin, *Nature Mater.*, 2016, 15, 169-+.
- K. A. See, J. A. Gerbec, Y. S. Jun, F. Wudl, G. D. Stucky and R. Seshadri, Adv. Energy Mater., 2013, 3, 1056-1061.
- M. C. Lin, M. Gong, B. Lu, Y. Wu, D. Y. Wang, M. Guan, M. Angell, C. Chen, J. Yang, B. J. Hwang and H. Dai, *Nature*, 2015, 520, 324-328.
- 23. Q. Li and N. J. Bjerrum, J. Power Sources, 2002, 110, 1-10.
- S. Yagi, T. Ichitsubo, Y. Shirai, S. Yanai, T. Soi, K. Murase and E. Matsubara, J. Mater. Chem. A, 2014, 2, 1144-1149.
- G. A. Elia, K. Marquardt, K. Hoeppner, S. Fantini, R. Y. Lin, E. Knipping, W. Peters, J. F. Drillet, S. Passerini and R. Hahn, *Adv. Mater.*, 2016, 28, 7564-7579.
- T. Gao, X. G. Li, X. W. Wang, J. K. Hu, F. D. Han, X. L. Fan, L. M. Suo, A. J. Pearse, S. B. Lee, G. W. Rubloff, K. J. Gaskell, M. Noked and C. S. Wang, *Angew. Chem. Int. Ed.*, 2016, 55, 9898-9901.
- M. Angell, C. J. Pan, Y. Rong, C. Yuan, M. C. Lin, B. J. Hwang and H. J. Dai, *Proc. Natl Acad. Sci. USA*, 2017, **114**, 834-839.
- S. Liu, J. J. Hu, N. F. Yan, G. L. Pan, G. R. Li and X. P. Gao, *Energy Environ. Sci.*, 2012, 5, 9743-9746.
- S. Liu, G. L. Pan, G. R. Li and X. P. Gao, J Mater. Chem. A, 2015, 3, 959-962.
- Z. Li, K. Xiang, W. T. Xing, W. C. Carter and Y. M. Chiang, Adv. Energy Mater., 2015, 5, 141410.
- 31. Ger. Offen. (1983), DE 3202265 Ger. Offen. (1983), DE 3202265
- 32. H. N. Holmes, J. Chem. Educ., 1930, 7, 233-244.
- M. Armand, F. Endres, D. R. MacFarlane, H. Ohno and B. Scrosati, *Nat. Mater.*, 2009, 8, 621-629.
- 34. G. A. Giffin, J Mater. Chem. A, 2016, 4, 13378-13389.
- 35. D. R. MacFarlane, M. Forsyth, P. C. Howlett, M. Kar, S. Passerini, J. M. Pringle, H. Ohno, M. Watanabe, F. Yan, W. J. Zheng, S. G. Zhang and J. Zhang, *Nature Rev. Mater.*, 2016, 1.
- 36. X. G. Sun and S. Dai, Electrochimica Acta, 2010, 55, 4618-4626.
- X. G. Sun, C. Liao, N. Shao, J. R. Bell, H. Luo, D. E. Jiang and S. Dai, *J. Power Sources* 2013, 237, 5-12.
- 38. J. S. Wilkes, J. A. Levisky, R. A. Wilson and C. L. Hussey, *Inorg. Chem.*, 1982, **21**, 1263-1264.
- Q. Liao, W. R. Pitner, G. Stewart, C. L. Hussey and G. R. Stafford, J. Electrochem. Soc., 1997, 144, 936-943.
- 40. Y. G. Zhao and T. J. VanderNoot, Electrochimica Acta, 1997, 42, 3-13.
- 41. F. H. Hurley and T. P. Weir, J. Electrochem. Soc., 1951, 98, 207-212.
- 42. L. D. Reed and E. Menke, J. Electrochem. Soc., 2013, 160, A915-A917.
- X. G. Sun, Z. H. Bi, H. S. Liu, Y. X. Fang, C. A. Bridges, M. P. Paranthaman, S. Dai and G. M. Brown, *Chem. Commun.*, 2016, 52, 1713-1716.
- H. M. Abood, A. P. Abbott, A. D. Ballantyne and K. S. Ryder, *Chem. Commun.*, 2011, 47, 3523-3525.
- 45. F. Endres, Chemphyschem, 2002, 3, 144-154.
- 46. S. Z. El Abedin and F. Endres, Chemphyschem, 2006, 7, 58-61.
- A. P. Abbott, R. C. Harris, Y.-T. Hsieh, K. S. Rydera and I. W. Sun, *Phys. Chem. Chem. Phys.*, 2014, 16, 14675-14681.
- 48. F. Coleman, G. Srinivasan and M. Swadzba-Kwasny, *Angew. Chem. Int. Ed.*, 2013, **52**, 12582-12586.
- Y. Nakayama, Y. Senda, H. Kawasaki, N. Koshitani, S. Hosoi, Y. Kudo, H. Morioka and M. Nagamine, *Phys. Chem. Chem. Phys.*, 2015, 17, 5758-5766.
- L. Legrand, A. Tranchant and R. Messina, J Electrochem. Soc., 1994, 141, 378-382.
- 51. L. Legrand, M. Heintz, A. Tranchant and R. Messina, *Electrochimica Acta*, 1995, 40, 1711-1716.
- Y. X. Fang, X. G. Jiang, X. G. Sun and S. Dai, *Chem. Commun.*, 2015, 51, 13286 – 13289.

 Y. X. Fang, K. Yoshii, X. G. Jiang, X. G. Sun, T. Tsuda, N. Mehio and S. Dai, *Electrochimica Acta*, 2015, 160, 82-88.

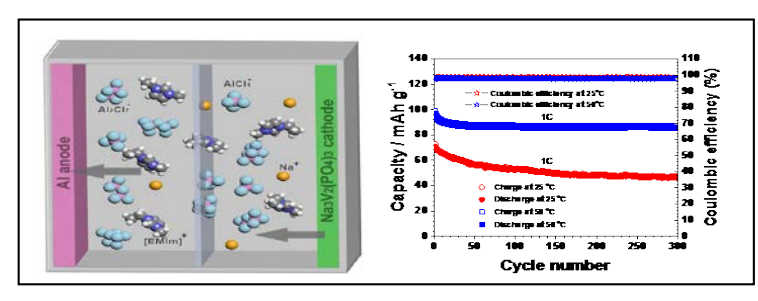
- X. G. Sun, Y. X. Fang, X. G. Jiang, K. Yoshii, T. Tsuda and S. Dai, *Chem. Commun.*, 2016, 52, 292 – 295.
- H. L. Wang, S. C. Gu, Y. Bai, S. Chen, N. Zhu, C. Wu and F. Wu, J Mater. Chem. A, 2015, 3, 22677-22686.
- M. P. Paranthaman, H. Liu, X. G. Sun, S. Dai and G. M. Brown, in Advances in batteries for medium and large-scale energy storage, eds. C. Menictas, M. Skyllas-Kazacos and T. M. Lim, Woodhead Publishing Ltd., 2015, ch. 13, pp. 463-474.
- N. Jayaprakash, S. K. Das and L. A. Archer, *Chem. Commun.*, 2011, 47, 12610–12612.
- H. L. Wang, Y. Bai, S. Chen, X. Y. Luo, C. Wu, F. Wu, J. Lu and K. Amine, Acs Appl. Mater. Interfaces, 2015, 7, 80-84.
- W. Wang, B. Jiang, W. Xiong, H. Sun, Z. Lin, L. Hu, J. Tu, J. Hou, H. Zhu and S. Jiao, *Sci. Rep.*, 2013, 3, 3383.
- L. X. Geng, G. C. Lv, X. B. Xing and J. C. Guo, Chem. Mater., 2015, 27, 4926-4929.
- B. Lee, H. R. Lee, T. Yim, J. H. Kim, J. G. Lee, K. Y. Chung, B. W. Cho and S. H. Oh, *J Electrochem. Soc.*, 2016, **163**, A1070-A1076.
- L. D. Reed, S. N. Ortiz, M. Xiong and E. J. Menke, *Chem. Commun.*, 2015, 51, 14397-14400.
- 63. N. S. Hudak, J. Phys. Chem. C, , 2014, 118, 5203-5215.
- J. V. Rani, V. Kanakaiah, T. Dadmal, M. S. Rao and S. Bhavanarushi, J. Electrochem. Soc., 2013, 160, A1781–A1784.
- H. B. Sun, W. Wang, Z. J. Yu, Y. Yuan, S. Wang and S. Q. Jiao, *Chem. Commun.*, 2015, 51, 11892-11895.
- M. Walter, K. V. Kraychyk, M. Ibanez and M. V. Koyalenko, *Chem. Mater.*, 2015, 27, 7452-7458.
- H. Dong, Y. Li, Y. Liang, G. Li, C. J. Sun, Y. Ren, Y. Lu and Y. Yao, *Chem. Commun.*, 2016, 52, 8263-8266.
- Y. A. Xu, Q. L. Wei, C. Xu, Q. D. Li, Q. Y. An, P. F. Zhang, J. Z. Sheng, L. Zhou and L. Q. Mai, Adv. Energy Mater., 2016, 6, 1600389.
- X. H. Rui, W. P. Sun, C. Wu, Y. Yu and Q. Y. Yan, Adv. Mater., 2015, 27, 6670-+.
- Z. Jian, W. Han, X. Lu, H. Yang, Y.-S. Hu, J. Zhou, Z. Zhou, J. Li, W. Chen, D. Chen and L. Chen, Adv. Energy Mater., 2013, 3, 156-160.
- Z. Jian, L. Zhao, H. Pan, Y.-S. Hu, H. Li, W. Chen and L. Chen, *Electrochem. Commun.*, 2012, 14, 86-89.
- H. Tokuda, K. Hayamizu, K. Ishii, M. Susan and M. Watanabe, *J Phys. Chem. B*, 2004, **108**, 16593-16600.
- H. Tokuda, K. Hayamizu, K. Ishii, M. Susan and M. Watanabe, *J Phys. Chem. B*, 2005, **109**, 6103-6110.
- H. Tokuda, K. Ishii, M. Susan, S. Tsuzuki, K. Hayamizu and M. Watanabe, *J Phys. Chem. B*, 2006, **110**, 2833-2839.
- M. Hagen, D. Hanselmann, K. Ahlbrecht, R. Maca, D. Gerber and J. Tubke, Adv. Energy Mater., 2015, 5, 1401986.
- W. X. Song, X. B. Ji, J. Chen, Z. P. Wu, Y. R. Zhu, K. F. Ye, H. S. Hou, M. J. Jing and C. E. Banks, *Phys. Chem. Chem. Phys.*, 2015, 17, 159-165.
- T. Jiang, G. Chen, A. Li, C. Z. Wang and Y. J. Wei, J Alloys Compd., 2009, 478, 604-607.
- R. K. B. Gover, A. Bryan, P. Burns and J. Barker, Solid State Ionics, 2006, 177, 1495-1500.
- M. Bianchini, N. Brisset, F. Fauth, F. Weill, E. Elkaim, E. Suard, C. Masquelier and L. Croguennec, *Chem. Mater.*, 2014, 26, 4238-4247.
- M. Bianchini, F. Fauth, N. Brisset, F. Weill, E. Suard, C. Masquelier and L. Croguennec, *Chem. Mater.*, 2015, 27, 3009-3020.

# A Novel Sodium-Aluminum Hybrid Battery

Xiao-Guang Sun,<sup>a\*</sup> Zhizhen Zhang,<sup>b</sup> Hongyu Guang,<sup>c</sup> Craig A. Bridges,<sup>a</sup> Youxing Fang,<sup>ad</sup> Yong-Sheng Hu,<sup>b\*</sup> Gabriel M. Veith,<sup>e</sup> Sheng Dai <sup>ad\*</sup>

**Keyword:** Aluminum battery, Na<sub>3</sub>V<sub>2</sub>(PO<sub>4</sub>)<sub>3</sub>, sodium battery, hybrid battery, ionic liquid

# **TOC**



A hybrid battery based on an aluminum anode, a sodium insertion cathode Na<sub>3</sub>V<sub>2</sub>(PO<sub>4</sub>)<sub>3</sub>, and a sodium/aluminum dual salt electrolyte has been demonstrated. The hybrid battery exhibits a discharge voltage of 1.25 V and a cathodic capacity of 99 mAh g<sup>-1</sup> under a current rate of C/10. It also shows good rate performance and long cycling

stability while maintaining a high coulombic efficiency of 98 %.